1   <u>Supporting Information (SI)</u>

2 Coupled Effect of Sulfidation and Ferrous

3 Dosing on Selenate Removal by Zerovalent

4 Iron Under Aerobic Conditions

5   Peng Fan,[†,‡,§] Yuankui Sun,[†,‡,§] Baoxue Zhou,[‡,||] Xiaohong Guan[†,‡,§]*

6   [†]State Key Laboratory of Pollution Control and Resources Reuse, College of Environmental

7   Science and Engineering, Tongji University, Shanghai 200092, China

8   [‡]Shanghai Institute of Pollution Control and Ecological Security, Shanghai 200092, China

9   [§]International Joint Research Center for Sustainable Urban Water System, Tongji

10   University, Shanghai 200092, China

11   [||]School of Environmental Science and Engineering, Shanghai Jiao Tong University,

12   Shanghai 200240, China

13   *Author to whom correspondence should be addressed

14   Xiaohong Guan, email: guanxh@tongji.edu.cn; phone: +86-21-65983869

15   **Prepared for *Environmental Science & Technology***

16   Number of pages (including this page): 34

17   Number of Texts: 8

18   Number of Figures: 16

19   Number of Tables: 2

Summary

43   removal rate (b, d) due to sulfidation or Fe^{2+} dosing for the pristine ZVI.

44   (Page S21)

45   **Figure S7.** Promotion factors for the amount of removed Se(VI) (a, c) and initial

46   removal rate (b, d) due to sulfidation or Fe^{2+} dosing in S-ZVI/Fe^{2+} system.

47   (Page S22)

48   **Figure S8.** X-ray diffraction scans of ZVI precipitates reacted with Se(VI) in ZVI,

49   ZVI/Fe^{2+}, S-ZVI, and S-ZVI/Fe^{2+} systems at different reaction time. (Page

50   S23)

51   **Figure S9.** SEM images of ZVI precipitates reacted with Se(VI) in ZVI, ZVI/Fe^{2+},

52   S-ZVI, and S-ZVI/Fe^{2+} systems. (Page S24)

53   **Figure S10.** Influence of Fe^{2+} dosing on variation of pH values during Se(VI)

54   removal by ZVI or S-ZVI. (Page S25)

55   **Figure S11.** Influence of Fe^{2+} dosing on the kinetics of Se(VI) removal by ZVI and

56   S-ZVI at pH 5.5. (Page S26)

57   **Figure S12.** X-ray diffraction scans of ZVI precipitates reacted with 50.0 or 100

58   mg/L Se(VI) in ZVI, ZVI/Fe^{2+}, S-ZVI, and S-ZVI/Fe^{2+} systems. (Page S27)

59   **Figure S13.** Variations of Fe^{2+} concentrations in the ZVI/Fe^{2+} and S-ZVI/Fe^{2+}

60   systems at different initial Se(VI) concentrations. (Page S28)

61   **Figure S14.** Real-time photos of solutions after Se(VI) reacted with (a) ZVI,

62   ZVI/Fe^{2+}, S-ZVI, and S-ZVI/Fe^{2+} systems at 12 h; (b) S-ZVI and S-ZVI/Fe^{2+}

63   systems at 2 h and 6 h. (Page S29)

64   **Figure S15.** Fe *K*-edge EXAFS spectra (a) and Fe k^3-weighted EXAFS spectra (b) of

65   S-ZVI samples reacted with Se(VI) for different durations without and with

74   **Text S1.** Details of materials using in this study.

75   Seven types of ZVI samples were used in this study and they were named to be

76   Alfa (supplied by Alfa Aesar Chemical Reagent Co.), Aladdin (supplied by Aladdin

77   Chemical Co.), Aldrich (supplied by Aldrich Chemical Co.), Macklin (supplied by

78   Macklin Chemical Co.), Sinopharm (supplied by Sinopharm Chemical Reagent Co.),

79   Tianjin (supplied by Tianjin Fengchuan Chemical Reagent Technologies Co.), and

80   Weifang (supplied by Weifang Kaihong Metal Products Co.), respectively. S-ZVI

81   with a S/Fe molar ratio of 0.05 was synthesized following the ball-milling method

82   employed in our previous studies, and the S/Fe molar ratio (0.05) was selected

83   because it was determined to be the optimum value for sequestering either Cr(VI) or

84   Se(VI) under aerobic conditions in prior studies.[1, 2] In brief, 5.0 g of pristine ZVI was

85   mixed with 0.1429 g sulfur powder to achieve the S/Fe molar ratios of 0.05. The

86   mixture was milled in a planetary ball mill (Boyuntong Instrument Technology,

87   Nanjing, China) with stainless steel jars (100 mL) and stainless steel balls (15 balls

88   with 10 mm in diameter and 80 balls with 6 mm in diameter in one jar). The milling

89   was performed at 500 rpm and at room temperature (Change of temperature was not

90   detected during milling). In particular, the ball-milled ZVI without adding elemental S

91   was also fabricated for comparison. After ball-milling for 4 h, the obtained S-ZVI

92   samples were freeze-dried for 24 h and then stored in a N_2-filled glovebox (Mikrouna,

93   china) for subsequent characterization and use. To explore the influence of Fe^{2+}

94   dosing, $FeCl_2 \cdot 4H_2O$ was added simultaneously into the working solution with ZVI or

95   S-ZVI particles. $FeCl_2 \cdot 4H_2O$ dissolved in the solution instantly and thus had no

96 effects on the surface area of ZVI or S-ZVI before the reaction. Sodium selenate

97 (Na_2SeO_4) was supplied by the Xiya Reagent Company. The other chemical reagents

98 were purchased from the Sinopharm Chemical Reagent Company. All chemicals were

99 obtained at the available highest purity and were used as received. All solutions were

100 prepared with ultrapure water generated from a Milli-Q system. Stock solution of

101 1000 mg/L Se(VI) was prepared by dissolving Na_2SeO_4 in ultrapure water.

102   **Text S2.** Experimental procedures of this study.

103   A typical test was initiated by adding 0.25 g ZVI or S-ZVI particles into a 500

104   mL working solution at 25 $^{\circ}$C, open to the air. To explore the influence of Fe^{2+} dosing

105   on Se(VI) removal by ZVI or S-ZVI, 0.50 mM $FeCl_2 \cdot 4H_2O$ was added

106   simultaneously into the working solution with ZVI or S-ZVI particles. Then the

107   solution was mixed with a propeller agitator (D2004W, Shanghai Sile Instrument Co.

108   Ltd.) at 400 rpm. At selected time intervals, a suspension of 5.0 mL was withdrawn

109   and immediately passed through a 0.22 μm membrane filter, and then acidified with

110   40 μL HNO_3 for analysis. After the batch tests, the reacted ZVI or S-ZVI precipitates

111   were collected, washed with ultrapure water for 3 times, freeze-dried in vacuum, and

112   then kept in a glove box for the subsequent characterization.

Text S3. Determination of the molar quantities of Fe(0), Fe(II), and Fe(III).

In the solid phase, the molar quantity of Fe(0) was calculated as follows:

$$n_{Fe(0)} = (n_{Fe(0)_0} + n_{Fe(II)_0} - n_{Fe(II)_{aq}}) \cdot \frac{n_{Fe(0)_{sample}}}{n_{Fe(0)_{sample}} + n_{Fe(II)_{sample}} + n_{Fe(III)_{sample}}}$$

$n_{Fe(0)_{sample}}$, $n_{Fe(II)_{sample}}$, $n_{Fe(III)_{sample}}$ are the molar quantities in the solid samples measured by digestion method. $n_{Fe(0)_{sample}}$ was determined by measuring the volume of H_2 evolved upon particle digestion in concentrated HCl (5.0 M). $n_{Fe(II)_{sample}}$ was the difference between total dissolved Fe(II) concentration and the calculated content of Fe^0. $n_{Fe(III)_{sample}}$ was the disparity between the content of total Fe after sample dissolution in concentrated HCl and total Fe(II) concentration in the dissolved solution. The Fe(II) concentration was determined with the 1,10-phenanthroline colorimetric methods using a UV/visible spectrophotometer (TU-1901, Purkinje General Instrument) at 510 nm and the concentration of total Fe was determined with Atomic Absorption Spectroscopy (Thermo Fisher Scientific iCE 3300 AAS). The molar quantities of Fe(II) and Fe(III) in the solid phase were calculated using the similar formula.

In the aqueous solution, the molar quantities of Fe(II) and Fe(III) were calculated as follows:

$$n_{Fe(II)} = n_{Fe(II)_{aq}}$$

$$n_{Fe(III)} = n_{Fe_{tot, aq}} - n_{Fe(II)_{aq}}$$

$n_{Fe_{tot, aq}}$ was determined with AAS while $n_{Fe(II)_{aq}}$ was determined with UV/visible spectrophotometer.

134   **Text S4.** Details of characterizing the solid phase with X-ray absorption fine structure

135   (XAFS) analyses.

136   Fe K-edge and Se K-edge XAFS analyses were performed with Si(111) crystal

137   monochromators at the BL14W Beam line at the Shanghai Synchrotron Radiation

138   Facility (SSRF) (Shanghai, China). Before the analysis at the beamline, samples were

139   placed into aluminum sample holders and sealed using Kapton tape film. Particular

140   care was taken to minimize the beam-induced oxidation of the samples by placing the

141   sample stands filled with reacted ZVI samples in a nitrogen-filled glove box for 6

142   hours before transferring them to zippered bags in this glove box. The XAFS spectra

143   were recorded at room temperature using a 4-channel Silicon Drift Detector (SDD)

144   Bruker 5040. Fe K-edge extended X-ray absorption fine structure (EXAFS) spectra

145   were recorded in transmission mode while Se K-edge X-ray absorption near edge

146   structure (XANES) spectra were recorded in fluorescence mode. Negligible changes

147   in the line-shape and peak position of Fe and Se K-edge XANES spectra were

148   observed between two scans taken for a specific sample. The oxidation states of Se in

149   solid phase were analyzed by linear combination fitting (LCF) using reference

150   compounds of Se powder (Se^0), Na_2SeO_3 (Se(IV)), and Na_2SeO_4 (Se(VI)). The major

151   species of Fe in Se-treated ZVI corrosion products were also quantified by LCF using

152   the collection of reference materials including metallic Fe (Fe^0), maghemite

153   ($\gamma\text{-}Fe_2O_3$), goethite ($\alpha\text{-}FeOOH$), lepidocrocite ($\gamma\text{-}FeOOH$), ands magnetite (Fe_3O_4).

154   The XAFS spectra of these standard samples were recorded in transmission mode.

155   The spectra were processed and analyzed by the software codes Athena.

156   S *K*-edge XANES spectra were recorded at the Beijing Synchrotron Radiation

157   Facility (BSRF), Beijing, China. The storage ring operated at 2.5 GeV with electron

158   currents between 100–200 mA. The Si(111) crystals of the fixed-exit double-crystal

159   monochromator were used to produce a monochromatic photon beam. The spectra

160   were recorded at a step width of 1 eV in an energy interval from 2465 to 2490 eV in

161   fluorescence mode to provide the chemical information of S in the bulk of S-ZVI

162   before or after reaction with Se(VI). The reference samples were measured in

163   transmission mode and five spectra were averaged to increase the signal-to-noise ratio.

164   The spectra were processed and analyzed by the software Athena. The fractions of

165   various sulfur species in solid phase were determined by LCF using reference

166   compounds of sulfide (FeS), disulfide (FeS_2), elemental S, and sulfate (Na_2SO_4).

167   **Text S5.** Determination of molar quantities of S(−II), S (−I), S(0), S(VI), Se(0),

168   Se(IV), and Se(VI).

169   The fractions of S(−II), S(−I), S(0), and S(VI) in the solid phase were quantified

170   based on the S K-edge XANES spectra. In the solid phase, the molar quantity of S(0)

171   was calculated with the following equation:

172    $$n_{S(0)} = n_{S_{tot, 0}} \cdot r_{S(0)_{sample}}$$

173        $r_{S(0)_{sample}}$ is the ratio of S(0) in the solid samples. $n_{S_{tot, 0}}$ represents the molar

174   quantity of total S in the fabricated S-ZVI samples, which was measured by

175   carbon-sulfur analyzer (ELTRA CS800, Germany). The molar quantities of S(-II),

176   S(-I), and S(VI) in the solid phase were calculated using the similar formula.

177   In aqueous solution, various sulfur species including SO_4^{2-}, SO_3^{2-}, and $S_2O_3^{2-}$

178   were determined using an ion chromatography equipped with an Ion Pac AS19

179   analytical column (4 × 250 mm²) and an Ion Pac AG19 guard column (4 × 50 mm²)

180   (Thermo Scientific Dionex ICS-5000). It was found that negligible soluble

181   sulfur-containing anions existed in the solution.

182   The fractions of Se(VI), Se(IV), and Se(0) in the solid phase were derived from

183   the LCF of the Se K-edge XANES spectra. In the solid phase, the molar quantity of

184   Se(0) was calculated via the following equation:

185    $$n_{Se(0)} = n_{Se(VI)_0} \cdot (1 - \frac{C}{C_0}) \cdot a_{Se(0)}$$

186        $a_{Se(0)}$ stands for the fraction of Se(0) in precipitates derived from the LCF of Se

187   K-edge XANES spectra. $n_{Se(VI)_0}$ represents the initial molar quantity of Se(VI) in the

188   experiment (0.19 mM). $\frac{C}{C_0}$ represents the ratio of Se(VI) concentration at selected

189   reaction conditions. The molar quantities of Se(IV) and Se(VI) in the solid phase were

190   calculated using the similar formula.

191   Since Se(VI) was the only Se species detected in aqueous phase by

192   HPLC-ICP-MS, its molar quantity was calculated via the following equation:

193
$$n_{Se(VI)} = n_{Se(VI)_0} \cdot \frac{C}{C_0}$$

194   **Text S6.** Details of other analytical methods used in this study.

195   X-ray diffraction (XRD, DXR-8000, Rigaku) analyses of the precipitates were

196 conducted using a diffracted beam graphite monochromator and Cu radiation at 40 kV

197 and 40 mA, scanning in the 2θ range of 10-90° with a step size of 0.02° and a count

198 time of 2 s per step. The specific surface areas of the ZVI samples were determined

199 by nitrogen adsorption using the Brunauer-Emmet-Teller (BET) method

200 (Micrometrics ASAP 2020). The size distributions of the ZVI samples were

201 determined by a Mastersizer 3000 laser diffraction particle size analyzer. The

202 scanning electron microscope (SEM) images of the reacted ZVI samples were

203 collected with a Hitachi 4700 microscope (at 15 kV). The pH value of working

204 solution was monitored with a commercial electrode (INESA pHS-3C, JBP-607). The

205 concentrations of total Fe (Fe_{tot}) and total Se (Se_{tot}) in the aqueous sample were

206 determined with an atomic absorption spectrometer (Thermo Fisher Scientific iCE

207 3300 AAS). The speciation of Se(IV) and Se(VI) in aqueous phase was determined

208 with HPLC-ICP-MS (Agilent HPLC 1200-ICPMS 7700). The concentration of

209 dissolved Fe^{2+} in the solution was determined with the ferrozine method at the

210 wavelength of 510 nm using an ultraviolet-visible spectrophotometer (Purkinje

211 TU-1902).

212 **Text S7.** Details of the calculating method of k.

213   Since all reactions have reached the equilibrium at the end of reaction in Figure

214 S1 (12 h for 5.0 and 10.0 mg/L Se(VI), 48 h for 20.0 mg/L Se(VI), 72 h for 30.0, 50.0,

215 and 100 mg/L Se(VI)), the amount of Se(VI) removed at the end of reaction could be

216 regarded as that removed at equilibrium. The theoretical value of $Q_{removal-half}$ can be

217 calculated with the following equation:

$$Q_{removal-half} = \frac{Q_{removal-final}}{2}$$

218   where $Q_{removal-final}$ represents the amount of Se(VI) removed at the end of the

219 reaction. The difference between the theoretical value of $Q_{removal-half}$ and of the amount

220 of Se(VI) removed at different time intervals was compared, and the real value of

221 $Q_{removal-half}$ (referred to $Q'_{removal-half}$ herein) is determined when the minimum value is

222 obtained. t'_{half} is the time point corresponding to $Q'_{removal-half}$, and k_r can be calculated

223 with the following equation in this study.

$$k_r = \frac{Q'_{removal-half}}{t'_{half}}$$

224

225 **Text S8.** Details of the calculating method of electron efficiency of reductants (EER).

226   EER, defined as the percentage of electrons transferred to the target contaminant

227 over the amount of electrons donated by ZVI and other reductants, if there are any, is

228 used to assess the selectivity of reductants toward target contaminant during reductive

229 removal of contaminant by ZVI system. The electrons provided by S and dosed Fe^{2+}

230 should be taken into account where S-ZVI and ZVI/Fe^{2+} was employed. Molar

231 quantities of S with various valence states in S-ZVI before and after the reaction with

232 Se(VI) were determined. The EER of bare ZVI, ZVI/Fe^{2+}, S-ZVI, and $S-ZVI/Fe^{2+}$

233 systems for Se(VI) sequestration can be calculated via equations 1 and 2, respectively.

234
$$\text{EER}(\%) = \frac{2n_{Se(IV)} + 6n_{Se(0)}}{3(n_{Fe(III)} - n'_{Fe(III)}) + 2(n_{Fe(II)} - n'_{Fe(II)})} \quad (1)$$

235
$$\text{EER}(\%) = \frac{2n_{Se(IV)} + 6n_{Se(0)}}{3(n_{Fe(III)} - n'_{Fe(III)}) + 2(n_{Fe(II)} - n'_{Fe(II)}) + 8(n_{S(VI)} - n'_{S(VI)}) + 2(n_{S(0)} - n'_{S(0)}) + (n_{S(-I)} - n'_{S(-I)})}$$

236 (2)

237   Where $n_{Se(IV)}$, $n_{Se(0)}$, $n_{Fe(III)}$, $n_{Fe(II)}$, $n_{S(VI)}$, $n_{S(0)}$ and $n_{S(-I)}$ are the molar quantities of

238 Se(IV), Se(0), Fe(III), Fe(II), S(VI), S(0), and S(−I) in both solid and liquid phases at

239 given reaction time, respectively. $n'_{Fe(III)}$, $n'_{Fe(II)}$, $n'_{S(VI)}$, $n'_{S(0)}$ and $n'_{S(-I)}$ stand for the

240 molar quantities of Fe(III), Fe(II), S(VI), S(0), and S(−I) in both solid and liquid

241 phases before the reaction, respectively. It should be specified that, the EER values

242 calculated using equations 1 and 2 are not the instantaneous electron efficiencies of

243 ZVI but are the mean values during the whole elapsed time. It should be noted that the

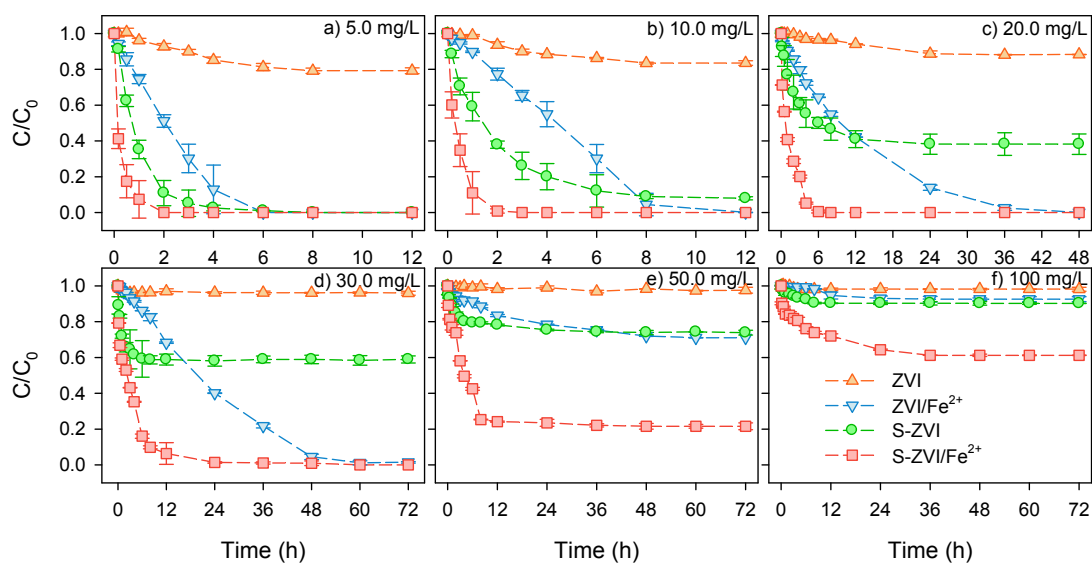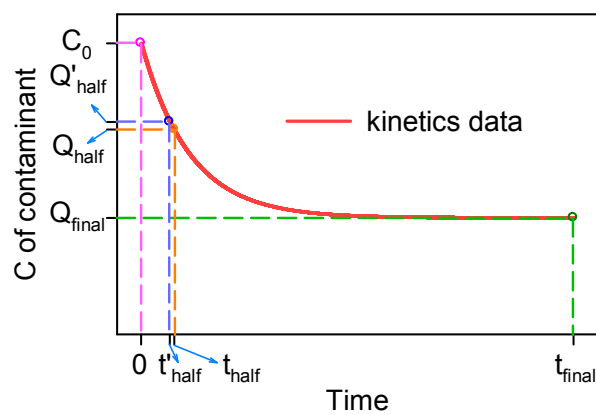244 EER values in ZVI, ZVI/Fe^{2+}, and S-ZVI systems were cited from our previous

245 study.[1]

246

Figure S1. Kinetics of Se(VI) removal by ZVI, ZVI/Fe^{2+}, S-ZVI, and S-ZVI/Fe^{2+} at different initial Se(VI) concentrations. Reaction conditions: pH_0 6.0, ZVI or S-ZVI = 0.50 g/L, $[Fe^{2+}]_0 = 0.50$ mM, Alfa ZVI.

250

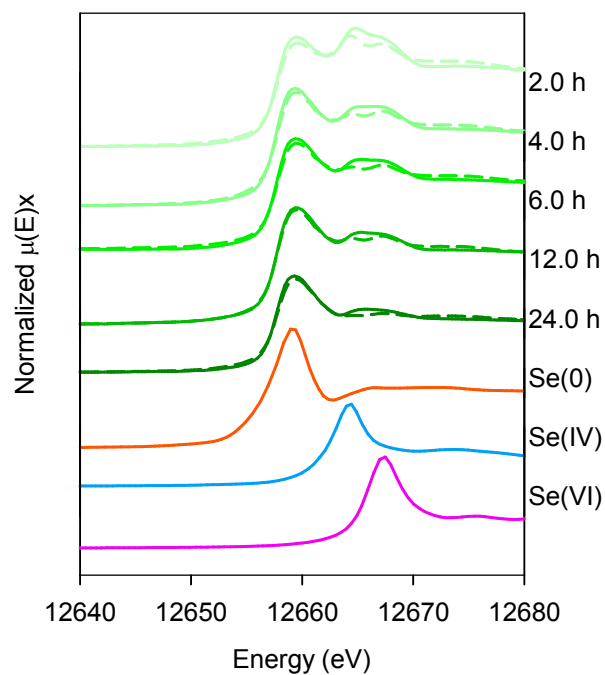251 **Figure S2**. Illustration of the parameters used in the calculation of k_r in this study.

252

Figure S3. Se K-edge XANES spectra of S-ZVI samples reacted with Se(VI) at pH_0 6.0 for different durations in S-ZVI/Fe^{2+} system. Experimental data are shown as thick solid lines and the dashed lines represent the LCF results. Reaction conditions: pH_0 6.0, $[Se(VI)]_0 = 30.0$ mg/L, S-ZVI = 0.50 g/L, $[Fe^{2+}]_0 = 0.50$ mM, Alfa ZVI.
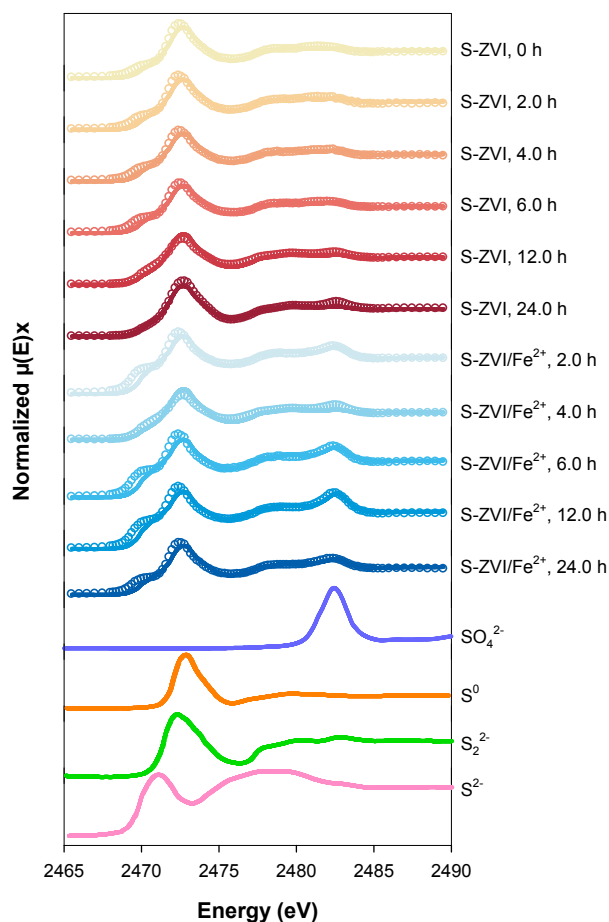
Figure S4. S *K*-edge XANES spectra of S-ZVI samples reacted with Se(VI) at pH_0 6.0 for different durations in S-ZVI and S-ZVI/Fe^{2+} systems. The circles and the thick solid lines represent the experimental data and the linear combination fits, respectively. Reaction conditions: pH_0 6.0, $[Se(VI)]_0 = 30.0$ mg/L, S-ZVI = 0.50 g/L, $[Fe^{2+}]_0 = 0.50$ mM, Alfa ZVI.
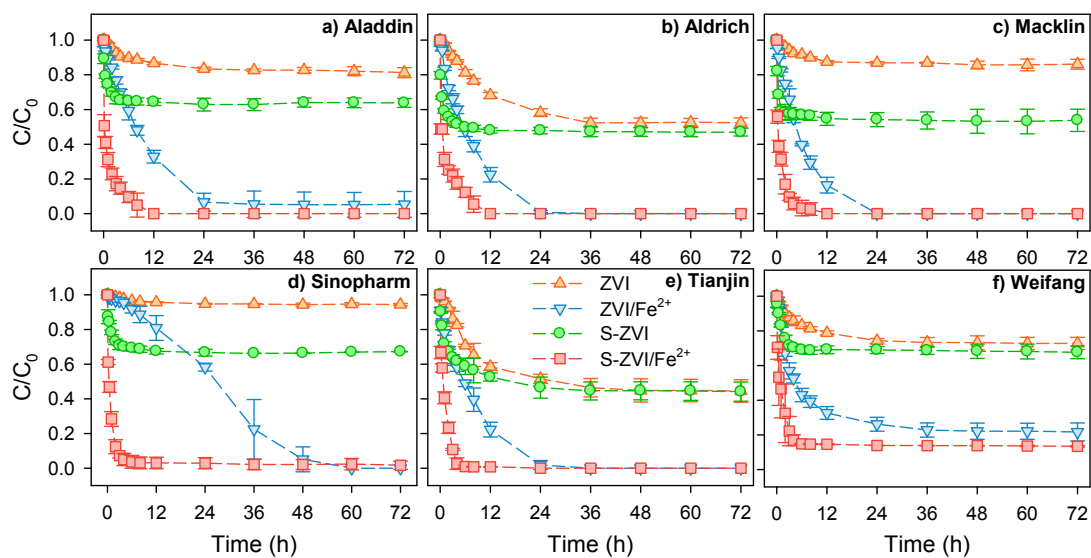
Figure S5. Kinetics of Se(VI) removal by ZVI, ZVI/Fe^{2+}, S-ZVI, and S-ZVI/Fe^{2+} systems, using 6 types of ZVI. Reaction conditions: pH$_0$ 6.0, ZVI = 0.50 g/L, [Se(VI)]$_0$ = 30.0 mg/L, [Fe^{2+}]$_0$ = 0.50 mM.
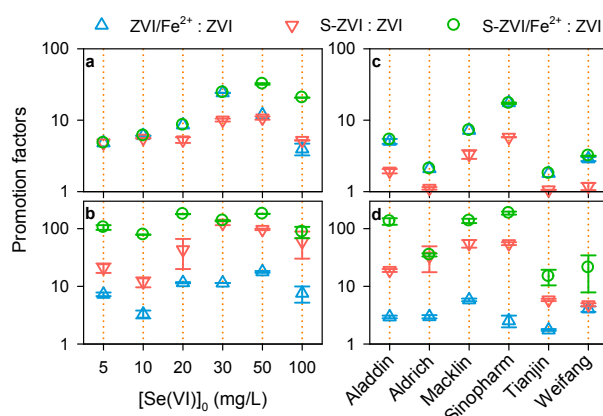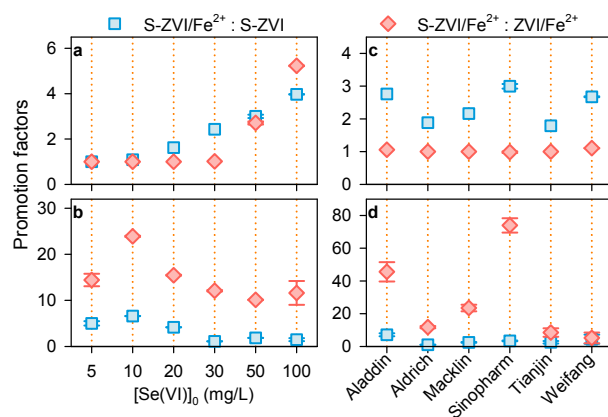
267

Figure S6. Promotion factors for the amount of removed Se(VI) (a, c) and initial removal rate (b, d) due to sulfidation or Fe^{2+} dosing for the pristine ZVI. Reaction conditions: pH_0 6.0, ZVI or S-ZVI = 0.50 g/L, (a–d) Alfa ZVI, (e–h) $[Se(VI)]_0$ = 30.0 mg/L.

272

Figure S7. Promotion factors for the amount of removed Se(VI) (a, c) and initial removal rate (b, d) due to sulfidation or Fe^{2+} dosing in S-ZVI/Fe^{2+} system. Reaction conditions: pH_0 6.0, ZVI or S-ZVI = 0.50 g/L, (a–d) Alfa ZVI, (e–h) $[Se(VI)]_0$ = 30.0 mg/L.
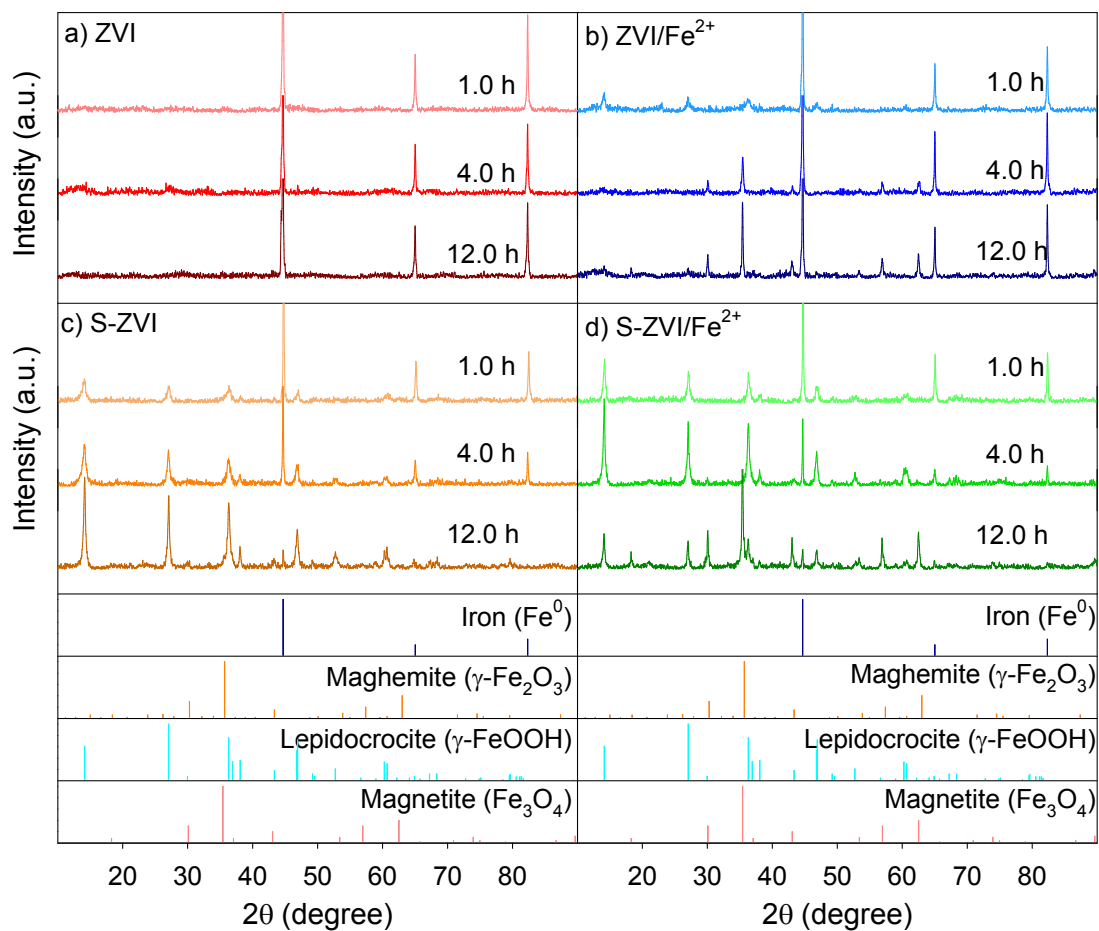
Figure S8. X-ray diffraction scans of ZVI precipitates reacted with Se(VI) in ZVI, ZVI/Fe^{2+}, S-ZVI, and S-ZVI/Fe^{2+} systems at different reaction time. Reaction conditions: pH_0 6.0, $[Se(VI)]_0$ = 30.0 mg/L, ZVI = 0.50 g/L, $[Fe^{2+}]_0$ = 0.50 mM, Alfa ZVI.
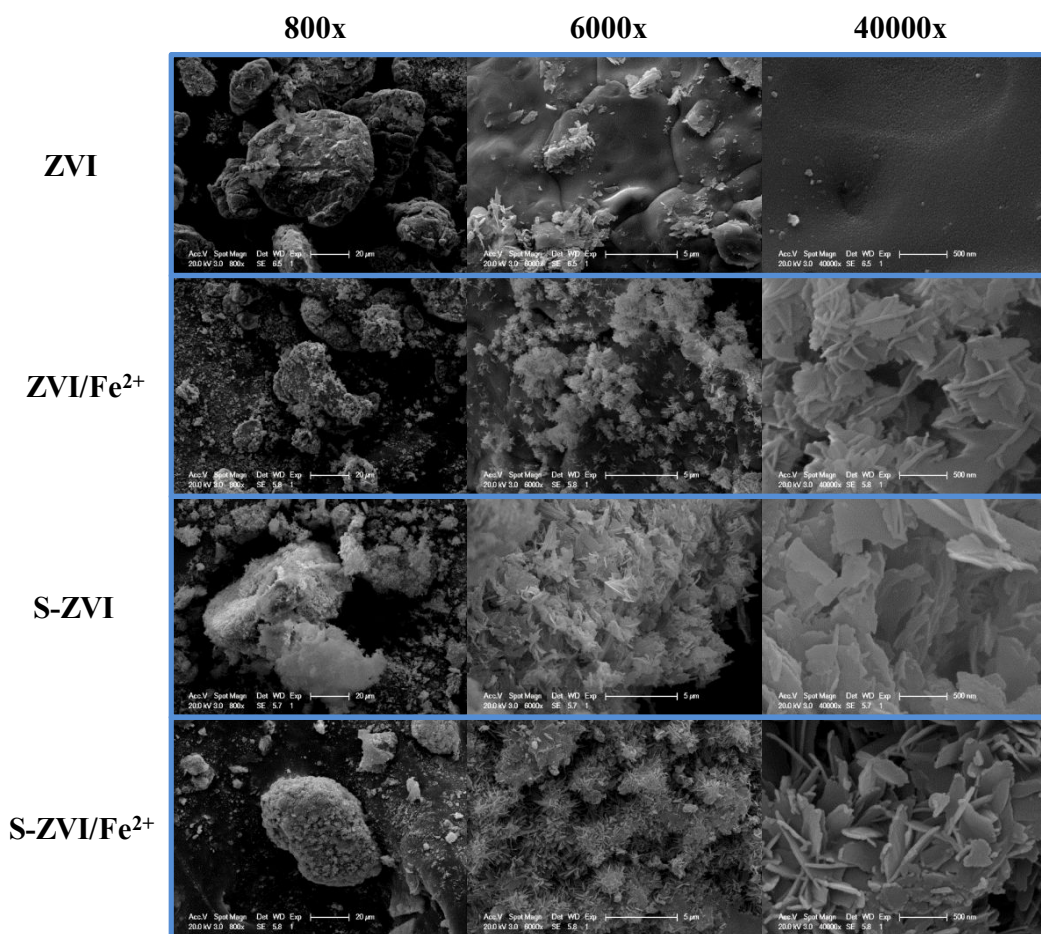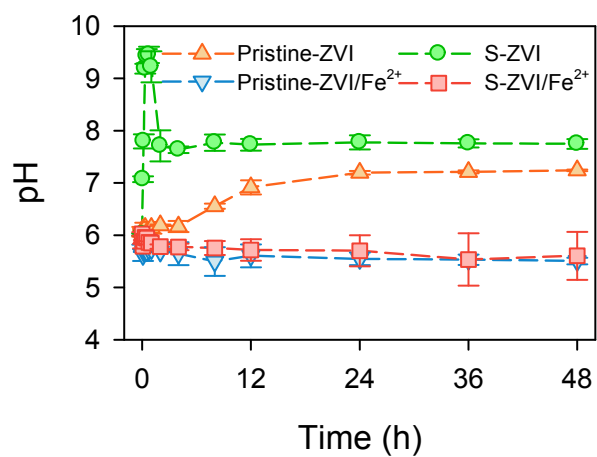
282

Figure S9. SEM images of ZVI precipitates reacted with Se(VI) in ZVI, ZVI/Fe^{2+}, S-ZVI, and S-ZVI/Fe^{2+} systems. 800x, 6000x, and 40000x represent the magnifications. Reaction conditions: pH$_0$ 6.0, [Se(VI)]$_0$ = 30.0 mg/L, ZVI = 0.50 g/L, reaction time = 12.0 h, [Fe^{2+}]$_0$ = 0.50 mM, Alfa ZVI.

287

Figure S10. Influence of Fe^{2+} dosing on variation of pH values during Se(VI) removal by ZVI or S-ZVI. Reaction conditions: pH_0 6.0, $[Se(VI)]_0 = 30.0$ mg/L, ZVI $= 0.50$ g/L, $[Fe^{2+}]_0 = 0.50$ mM, Alfa ZVI.
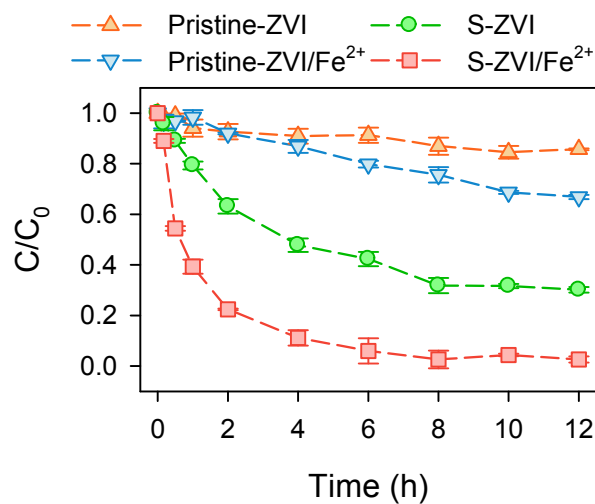
291

Figure S11. Influence of Fe^{2+} dosing on the kinetics of Se(VI) removal by ZVI and S-ZVI at pH 5.5. Reaction conditions: pH value of the reaction mixture was stabilized at 5.5 by manually adding HCl and/or NaOH, $[Se(VI)]_0 = 30.0$ mg/L, ZVI = 0.50 g/L, $[Fe^{2+}]_0 = 0.50$ mM, Alfa ZVI.
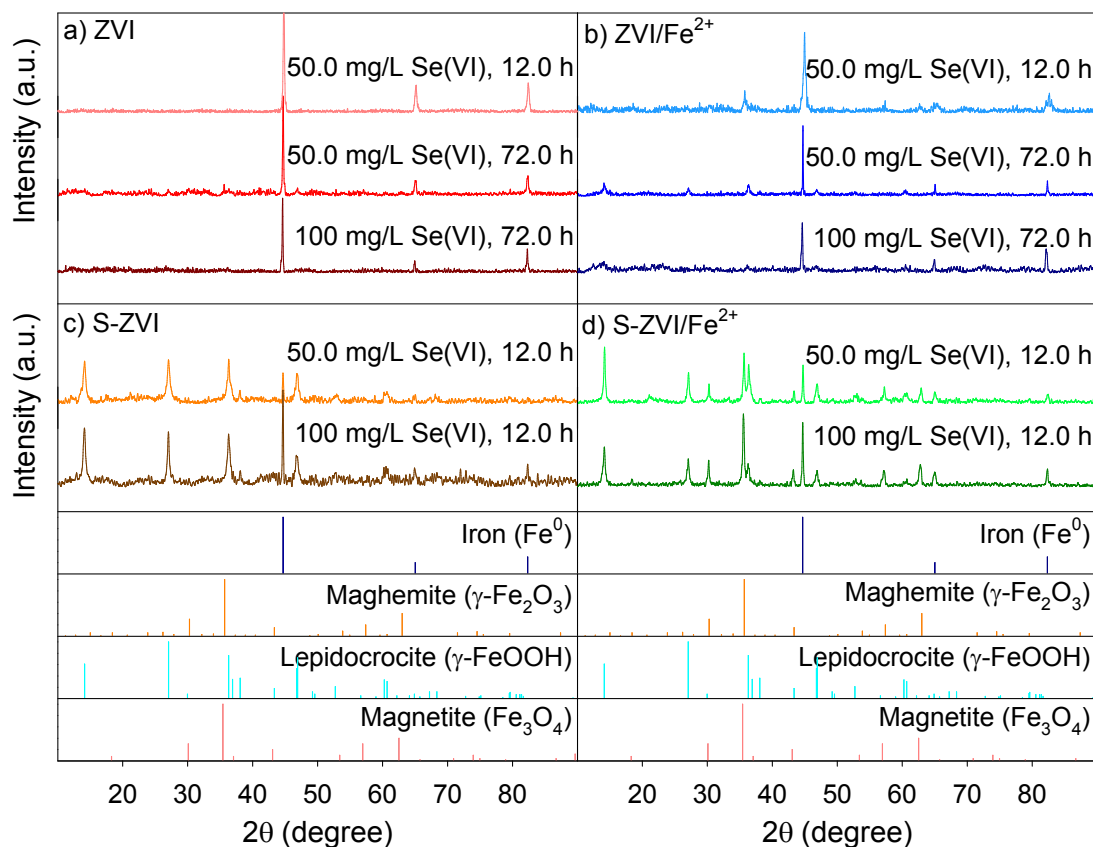
296

Figure S12. X-ray diffraction scans of ZVI precipitates reacted with 50.0 or 100

mg/L Se(VI) in ZVI, ZVI/Fe^{2+}, S-ZVI, and S-ZVI/Fe^{2+} systems. Reaction conditions:

pH_0 6.0, ZVI = 0.50 g/L, $[Fe^{2+}]_0$ = 0.50 mM, Alfa ZVI, reaction time = 12 or 72 h.
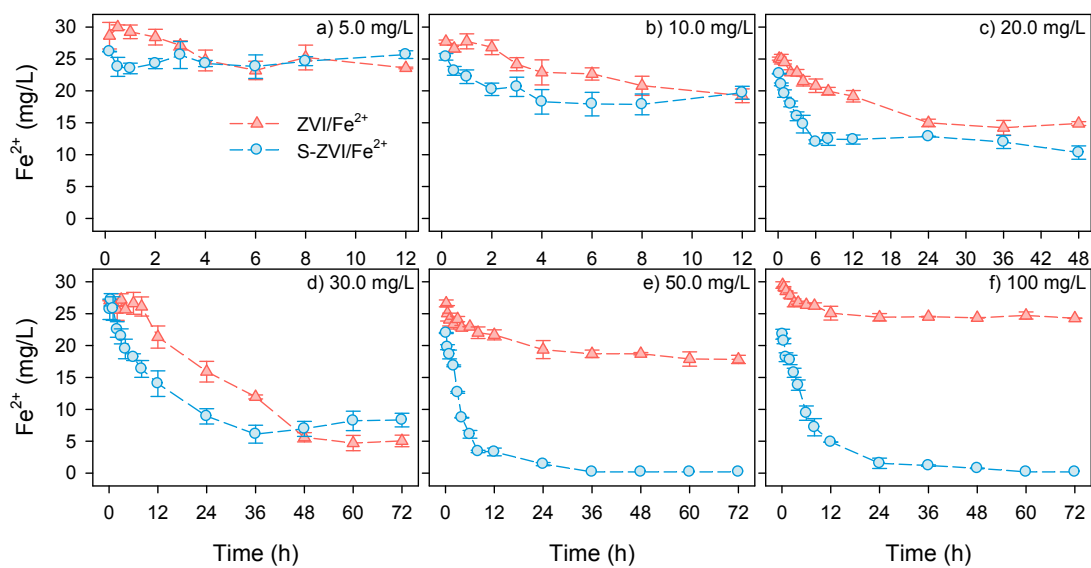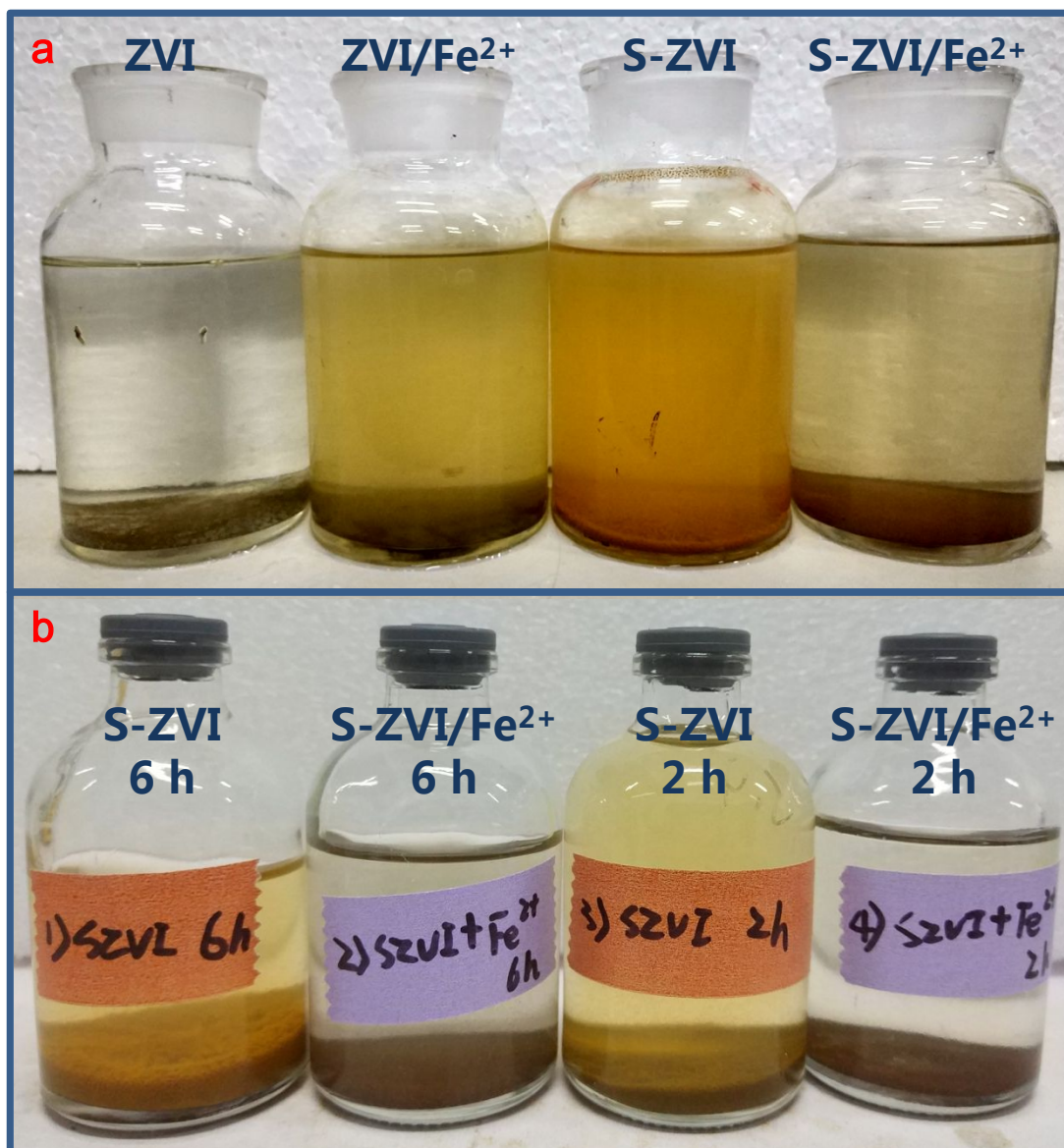
300

Figure S13. Variations of Fe^{2+} concentrations in the ZVI/Fe^{2+} and $S-ZVI/Fe^{2+}$
systems at different initial Se(VI) concentrations. Reaction conditions: pH_0 6.0, ZVI =
0.50 g/L, $[Fe^{2+}]_0$ = 0.50 mM, Alfa ZVI.

Figure S14. Real-time photos of solutions after Se(VI) reacted with (a) ZVI, ZVI/Fe^{2+}, S-ZVI, and S-ZVI/Fe^{2+} systems at 12.0 h; (b) S-ZVI and S-ZVI/Fe^{2+} systems at 2.0 h and 6.0 h. Reaction conditions: pH$_0$ 6.0, [Se(VI)]$_0$ = 30.0 mg/L, ZVI = 0.50 g/L, [Fe^{2+}]$_0$ = 0.50 mM, Alfa ZVI.

309

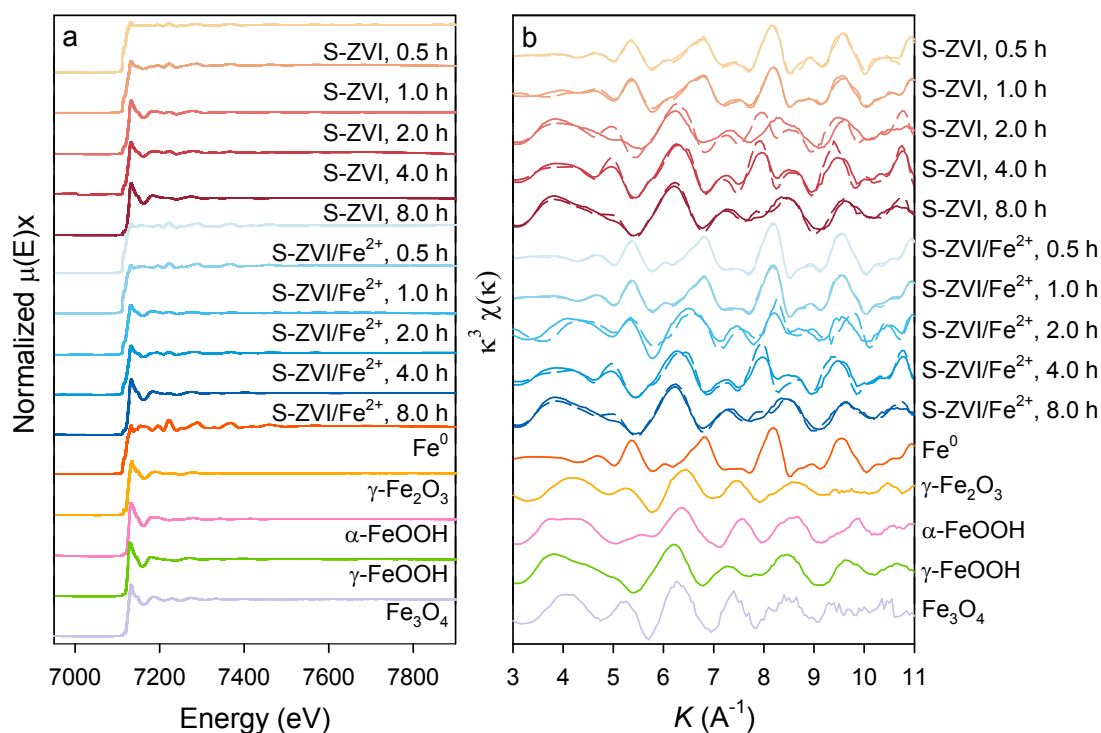**Figure S15.** Fe *K*-edge EXAFS spectra (a) and Fe k^3-weighted EXAFS spectra (b) of S-ZVI samples reacted with Se(VI) for different durations without and with Fe^{2+}. Experimental data are shown as the dashed lines and the solid lines represent the LCF results and the spectra of the reference materials in (b). Reaction conditions: pH_0 6.0, $[Se(VI)]_0 = 30.0$ mg/L, S-ZVI $= 0.50$ g/L, $[Fe^{2+}]_0 = 0.50$ mM, Alfa ZVI.
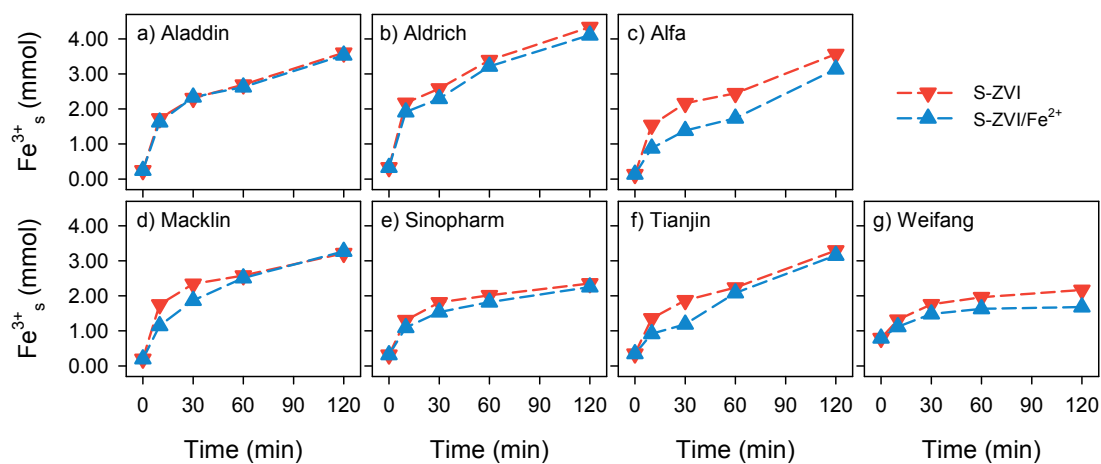
315

Figure S16. The variation of Fe^{3+} quantity in the solid phase of S-ZVI and S-ZVI/Fe^{2+} systems during Se(VI) removal, using 7 types of ZVI. Reaction conditions: pH_0 6.0, $[Se(VI)]_0 = 30.0$ mg/L, S-ZVI = 0.50 g/L, $[Fe^{2+}]_0 = 0.50$ mM.

319 **Table S1.** Summary of the properties of the ZVI and S-ZVI samples employed in this
320 study.

Origin	ZVI samples	Size/d_{50}, μm	SSA*/m^2 g^{-1}
Aladdin	ZVI	32.4	0.62
	S-ZVI	32.2	0.63
Aldrich	ZVI	119.4	0.12
	S-ZVI	49.9	0.20
Alfa	ZVI	46.2	0.47
	S-ZVI	28.8	0.92
Macklin	ZVI	38.6	0.55
	S-ZVI	35.1	0.61
Sinopharm	ZVI	40.5	0.15
	S-ZVI	33.8	0.42
Tianjin	ZVI	80.8	0.19
	S-ZVI	46.5	0.66
Weifang	ZVI	48.4	0.36
	S-ZVI	39.6	0.88

321 *SSA represent the specific surface area determined by the BET method.

System	Reaction time (h)	State	Amount of species (mmol)									
			Fe(0)	Fe(II)	Fe(III)	S(-II)	S(-I)	S(0)	S(VI)	Se(0)	Se(IV)	Se(VI)
S-ZVI	0	Solid	3.87	0.14	0.13	0.0655	0.0970	0.0488	0.0038	\	\	\
	2.0	Solid	0.79	0.05	3.05	0.0736	0.0889	0.0469	0.0057	0.0427	0.0132	0.0104
		Aqueous	0	0	0	0	0	0	0	0	0	0.1237
	4.0	Solid	0.39	0.28	3.21	0.0808	0.0798	0.0473	0.0073	0.0582	0.0147	0.0013
		Aqueous	0	0	0	0	0	0	0	0	0	0.1158
	6.0	Solid	0.23	0.33	3.32	0.0855	0.0707	0.0499	0.0090	0.0602	0.0153	0
		Aqueous	0	0	0	0	0	0	0	0	0	0.1144
	12	Solid	0.17	0.53	3.18	0.0862	0.0726	0.0438	0.0126	0.0674	0.0121	0
		Aqueous	0	0	0	0	0	0	0	0	0	0.1105
	24	Solid	0.02	0.44	3.42	0.0506	0.0977	0.0562	0.0107	0.0688	0.0107	0
		Aqueous	0	0	0	0	0	0	0	0	0	0.1104
S-ZVI/Fe^{2+}	2.0	Solid	0.9189	0.35	3.2367	0.1022	0.0550	0.0420	0.0160	0.0605	0.0279	0.0047
		Aqueous	0	0.20	0	0	0	0	0	0	0	0.0969
	4.0	Solid	0.4512	0.36	3.7014	0.0948	0.0572	0.0451	0.0181	0.0984	0.0252	0.0025
		Aqueous	0	0.20	0	0	0	0	0	0	0	0.0638
	6.0	Solid	0.2876	0.37	3.8632	0.1007	0.0516	0.0413	0.0216	0.1310	0.0307	0
		Aqueous	0	0.19	0	0	0	0	0	0	0	0.0282
	12	Solid	0.1685	0.59	3.7674	0.1055	0.0448	0.0407	0.0242	0.1552	0.0253	0
		Aqueous	0	0.18	0	0	0	0	0	0	0	0.0095
	24	Solid	0.0524	0.71	3.8441	0.0825	0.0604	0.0517	0.0206	0.1710	0.0190	0
		Aqueous	0	0.10	0	0	0	0	0	0	0	0

Reference

(1) Fan, P.; Li, L.; Sun, Y.; Qiao, J.; Xu, C.; Guan, X. Selenate removal by Fe^0 coupled with ferrous iron, hydrogen peroxide, sulfidation, and weak magnetic field: A comparative study. *Water Res.* **2019**, *159*, 375-384.

(2) Li, J.; Zhang, X.; Liu, M.; Pan, B.; Zhang, W.; Shi, Z.; Guan, X., Enhanced reactivity and electron selectivity of sulfidated zerovalent iron toward chromate under aerobic conditions. *Environ. Sci. Technol.* **2018,** *52* (5), 2988-2997.